

A selective inhibitor of the osteoclastic V-H⁺-ATPase prevents bone loss in both thyroparathyroidectomized and ovariectomized rats

Luciano Visentin,¹ Robert A. Dodds,² Maurizio Valente,¹ Paola Misiano,¹ Jeremy N. Bradbeer,² Sergio Oneta,¹ Xiaoguang Liang,² Maxine Gowen,² and Carlo Farina¹

¹SmithKline Beecham S.p.A, Milano, Italy

²SmithKline Beecham Pharmaceuticals, Bone and Cartilage Biology, King of Prussia, Pennsylvania, USA

Address correspondence to: Carlo Farina, SmithKline Beecham S.p.A., Via Zambelletti, 20021 Baranzate, Milano, Italy. Phone: 39-02-38062429; Fax: 39-02-38062606; E-mail: Carlo_Farina@sbphrd.com.

Received for publication December 28, 1998, and accepted in revised form June 14, 2000.

A potent and selective inhibitor of the osteoclastic V-H⁺-ATPase, (2Z,4E)-5-(5,6-dichloro-2-indolyl)-2-methoxy-N-(1,2,2,6,6-pentamethylpiperidin-4-yl)-2,4-pentadienamide (SB 242784), was evaluated in two animal models of bone resorption. SB 242784 completely prevented retinoid-induced hypercalcemia in thyroparathyroidectomized (TPTX) rats when administered orally at 10 mg/kg. SB 242784 was highly efficacious in the prevention of ovariectomy-induced bone loss in the rat when administered orally for 6 months at 10 mg/kg/d and was partially effective at 5 mg/kg/d. Its activity was demonstrated by measurement of bone mineral density (BMD), biochemical markers of bone resorption, and histomorphometry. SB 242784 was at least as effective in preventing bone loss as an optimal dose of estrogen. There were no adverse effects of compound administration and no effects on kidney function or urinary acidity. Selectivity of the inhibitor was further studied using an in situ cytochemical assay for bafilomycin-sensitive V-H⁺-ATPase using sections of osteoclastoma and numerous other tissues. SB 242784 inhibited the osteoclast enzyme at 1,000-fold lower concentrations than enzymes in any of the other tissues evaluated. SB 242784 demonstrates the utility of selective inhibition of the osteoclast V-H⁺-ATPase as a novel approach to the prevention of bone loss in humans.

J. Clin. Invest. 106:309-318 (2000).

Introduction

Inhibitors of bone resorption can preserve bone mass and maintain normal bone architecture, thereby preventing fractures in later life (1).

The bone-resorption process requires secretion of protons by the osteoclasts (2). This allows the dissolution of the bone mineral and the maintenance of the acidic environment required by proteolytic enzymes to degrade the bone matrix (3). Protons are extruded by a proton pump belonging to the class of vacuolar-type H⁺-ATPases (V-H⁺-ATPases (4) that is present in high concentration on the ruffled border (apical surface) of the resorbing osteoclast.

The osteoclast V-H⁺-ATPase therefore represents a previously unexploited molecular target for the design of novel agents for reducing osteoclast activity. However, since V-H⁺-ATPase is an ubiquitous component of eukaryotic organisms and is the major electrogenic pump of endomembranes (5), the selective inhibition of the osteoclast V-H⁺-ATPase must be achieved in order to afford novel drugs that may constitute useful and safe agents for the treatment of osteoporosis and related osteopenic diseases.

Bafilomycin A₁, a potent and specific inhibitor of V-H⁺-ATPases (6), inhibits bone resorption both in vitro (7) and in vivo (8). However, since bafilomycin is not selective for any particular type of V-H⁺-ATPases, when

administered to animals it inhibits all the essential V-H⁺-ATPases leading to systemic alteration of cellular physiology and to unacceptable toxicity (9).

Recently, a novel class of small molecules endowed with potent osteoclast V-H⁺-ATPase inhibitory activity has been discovered (10), whose optimization resulted in (2Z,4E)-5-(5,6-dichloro-2-indolyl)-2-methoxy-N-(1,2,2,6,6-pentamethylpiperidin-4-yl)-2,4-pentadienamide (SB 242784; Figure 1) (11).

The in vitro V-H⁺-ATPase inhibitory profile of SB 242784 has been reported previously (11). SB 242784 was a low-nanomolar inhibitor (IC₅₀ = 26.3 nM) of the bafilomycin-sensitive (vacuolar) Mg²⁺-ATPase in membrane preparations of osteoclasts obtained from egg-laying hens. In addition, SB 242784 was a very potent inhibitor of bone resorption (IC₅₀ = 3.4 nM) in an assay measuring the collagen fragments released from bone slices after a 48-hour incubation with human osteoclasts.

In this paper we characterize further the biochemical and pharmacological actions of SB 242784 and demonstrate that it is highly selective for the V-H⁺-ATPase of human osteoclasts when compared with V-H⁺-ATPases from a number of other human tissues. Most importantly, we show that oral administration of SB 242784 reduces the retinoid-induced hypercalcemia in thyroparathyroidectomized (TPTX) rats and prevents the

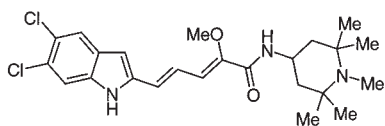


Figure 1
Chemical structure of SB 242784.

increased rate of bone resorption and the consequent bone loss that is observed in rats after ovariectomy.

Importantly, at fully active therapeutic doses, SB 242784 has no effect on urinary acid excretion. Since $V\text{-H}^+\text{-ATPase}$ located on the plasma membrane in kidneys participates in urinary acidification, this finding confirms *in vivo* the selectivity of SB 242784 measured *in vitro*.

Methods

In situ cytochemical Mg-ATPase assay. The cytochemical assay developed for determining $V\text{-ATPase}$ activity in tissue sections was derived from the method described by Chayen (12). The basis of the assay is the use of the phosphate-trapping agent lead ammonium citrate/acetate (LACA) complex. Free phosphate generated by endogenous enzymatic hydrolysis of exogenously added ATP (within individual cells of the tissue section) competes with ammonium citrate moieties and precipitates lead phosphate, which can be converted to a colored (brown/black) lead sulphide precipitate with ammonium sulphide.

Fresh, unfixed, 8- μm cryostat sections were preincubated for 15 minutes at 37°C in a 10% solution of Polypep 5115 in 0.2 M Tris buffer, pH 7.5, to remove free phosphate. The sections were incubated at 37°C for 10 minutes in reaction medium containing 4 mM ATP, 50 mM MgCl_2 , and 8 mg/mL LACA in 10% Polypep 5115 in 0.2 M Tris buffer, pH 7.5. All reagents were supplied by Sigma Chemical Co. (St. Louis, Missouri, USA). The assay was performed on serial sections containing increasing concentrations of bafilomycin (0, 0.001–10 nM) or SB 242784 (0, 0.005–50 μM). Serial sections were also assayed in the presence of 10 nM bafilomycin and 10 nM bafilomycin plus 50 μM SB 242784. Statistical analysis was done using an unpaired *t* test.

Reaction product was quantified using a Vickers M85 scanning and integrating microcytrophotometer, a spectrophotometer built around a microscope. This instrument facilitates the measurement of the amount of chromophore in individual cells using a disc of light visible to the operator but not the instrument photomultiplier. A spot of light of known wavelength is then sent through the objective and onto the specimen. This spot traverses the cell in a raster pattern and then passes on to the photomultiplier. The instrument then summates all measured absorptions for the area scanned. The spot takes measurements only within the area selected by the light disc. Using a filter of known absorbance, the absolute mean integrated extinction (MIE) can be determined for each cell. Thirty cells were measured in triplicate sets of sections of the following:

human and cynomolgus monkey kidney (proximal cells) and liver (hepatocytes); monkey brain; human spleen, stomach, heart, and giant cell tumor (rich in osteoclasts). Randomized measurements were recorded blind at distinct sites for each section with the instrument settings as follows: a mask size suitable for the specimen, a $\times 40$ objective, and a spot size of 0.5 μm at a wavelength of 580 nm.

Results are presented as $\text{MIE} \times 100 \pm \text{SEM}$, or expressed as percentage of control. In all cell types ATPase activity was substrate and magnesium dependent and linear with time for up to 30 minutes. The assay omits Na^+ or K^+ ions, and thus ouabain-sensitive (0.4 mM) $\text{Na}^+/\text{K}^+\text{-ATPase}$ activity within tissue sections was negligible. *L-p*-bromotetramisole oxalate (0.4 mM; specific inhibitor of alkaline phosphatase) had no inhibitory effect on ATPase activity.

Hypercalcemia induced by the retinoid Ro 13-6298 in TPTX rats

Animals/administration of test compounds. The method used was similar to that described by Trechsel (13). Male thyroparathyroidectomized (TPTX) Sprague-Dawley rats (Charles River, Calco, Italy), weighing 175–200 g, were maintained at $22 \pm 1^\circ\text{C}$, 12-hour light/dark cycle, fed with a standard diet (Mucedola No. 4RF21, Settimo Milanese, Milan, Italy) and water *ad libitum*. After a week of acclimatization, during which the animals received 1 μg thyroxin subcutaneously every other day, total plasma calcium was measured and only rats with calcium values less than 1.75 mM were considered TPTX. The TPTX rats were randomly divided into four groups of eight each and placed in single cages. Retinoid Ro 13-6298 was synthesized according to the procedure described by Loeliger (14) and was injected subcutaneously at the dose of 30 $\mu\text{g}/\text{rat}$ in 0.1 mL of polyethylene glycol 300 with 10% ethanol for 3 days to all animals. At the same time, SB 242784, suspended in 1% methylcellulose, was administered orally at doses of 2.5, 5, and 10 mg/kg, to groups 1–3 respectively, whereas group 4 received vehicle alone.

Analytical procedures. Blood samples were taken from the tail vein of all animals before and 4 days after the first treatment with retinoid plus test compound. Plasma was then obtained by centrifugation (4300 g for 10 minutes), and total calcium was measured by atomic absorption spectrophotometry (Varian A400; Varian Inc., Palo Alto, California, USA). Calcium plasma concentrations were expressed in millimolar.

Osteoporosis induced by ovariectomy in rats

Animals/administration of test compounds. Three-month-old female Sprague-Dawley rats (Charles River Italy), weighing 220–260 g, were maintained at $22 \pm 1^\circ\text{C}$, 12-hour light/dark cycle, fed with a standard diet (Mucedola No. 4RF21; Settimo Milanese) and water *ad libitum*. After a week of acclimatization, the animals were randomly divided into five groups of 10 each and

placed in individual metabolic cages to collect 24-hour urine samples for determination of urine volume, pH and total acidity, basal contents of pyridinoline (PYD) and deoxypyridinoline (DPD). During collection, to avoid urea degradation, urine samples were maintained frozen. Basal bone mineral density (BMD) of distal femur metaphysis and lumbar vertebrae (L3–L6, as total area) were evaluated. Four days later, under pentobarbitone anesthesia (35 mg/kg intravenously), animals were bilaterally ovariectomized (groups 1–4) or sham operated (group 5) (15, 16). Immediately after surgery, animals were treated with vehicle, estrogen, or SB 242784. Estrogen (group 1) was administered as slow-release pellets containing 2.5 mg of 17 β -estradiol (Innovative Research of America, Sarasota, Florida, USA); each animal was implanted subcutaneously with one pellet, which was replaced after 3 months. SB 242784 was administered by oral gavage at 5 and 10 mg/kg (groups 2 and 3, respectively), and 1% methocel vehicle was given orally to both ovariectomized and sham-operated rats (groups 4 and 5). All treatments were performed daily for 6 months. Urinary parameters, PYD and DPD determination, and evaluation of BMD were performed on a monthly basis for 6 months. Body weight of the animals was recorded throughout the experimental period.

Analytical procedures

Measurement of BMD. Determinations were performed using an Hologic QDR 1000 Plus (Hologic, Waltham, Massachusetts, USA) X-ray bone densitometer, complete with a 0.64-mm collimator, and using software specifically designed to measure BMD of small animals in vivo. The BMD values were expressed as grams per square centimeter.

Measurement of urinary excretion of PYD and DPD cross-links. According to the method of Eyre (17), 250- μ L urine samples were hydrolyzed with 12 N HCl at 110°C for 16 hours. Hydrolysates were then diluted with glacial acetic acid and *n*-butanol and applied to CF1 cellulose columns to extract the analytes. Samples were eluted with water, evaporated to dryness at 40°C in a centrifugal evaporator (Univapo 100H; UniEquip, Martinsried, Munich, Germany), and reconstituted in 250 μ L 1% heptafluorobutyric acid. A 50- μ L aliquot was injected into a C18 reverse-phase column (Supelco Inc., Bellefonte, Pennsylvania, USA) and, after an isocratic separation, fluorimetrically detected (250 nm excitation wavelength, 395 nm emission wavelength). The interassay coefficient of variation was 12.9% for PYD and 13.1% for DPD. The amounts of PYD and DPD were expressed as nanomoles per 24 hours.

Measurement of urine total acidity. Free acidity was evaluated by titrating urine samples with 0.01 M NaOH at pH 7.4. NH₄⁺ content was determined by enzymatic bioanalysis (Urea/Ammonia Kit; Boehringer Mannheim, Mannheim, Germany). Total acidity of urine was measured as the sum of free acidity and ammonium content and is expressed in equivalents per liter (*N*).

Histomorphometry

All animals received 10 mg/kg of calcein intraperitoneally, 13 and 4 days before necropsy. Bone samples were fixed, stained with Villanueva stain, dehydrated through increasing concentrations of ethanol, defatted in acetone, and embedded in methyl methacrylate (Polysciences, Inc., Warrington, Pennsylvania, USA). Longitudinal undecalcified sections (5 μ m) collected from three planes (separated by 100 μ m) of the proximal tibia were cut on a Leica microtome (SM2500S). Histomorphometric analysis was carried out using an Osteomeasure System (OsteoMetrics Inc., Atlanta, Georgia, USA), without knowledge of group allocation. Measurements were restricted to a mean tissue area of approximately 8 mm², beginning 1 mm below the epiphyseal growth plate. Primary measurements included area of bone and marrow (square millimeter), bone area (square millimeter), perimeter of bone (millimeter), single-labeled perimeter (sL.Pm; millimeter) and double-labeled perimeter (dL.Pm; millimeter), osteoid perimeter (O.Pm; millimeter), and eroded perimeter (Er.Pm; millimeter). Derived indices included trabecular bone volume (Tb.Ar; percentage), trabecular number (Tb.N; number per millimeter), trabecular thickness (Tb.Th; micrometer), trabecular separation (Tb.Sp; micrometer), bone formation rate with bone surface referent (BFR/BS; cubic micrometer per square micrometer per year), BFR/BV (bone area referent; percentage per year), BFR/TV (tissue area referent; percent per year), mineral apposition rate (MAR; micrometer per day), and percent of labeled perimeter (L.Pm; percentage).

Urinary acid excretion in acid-loaded rats

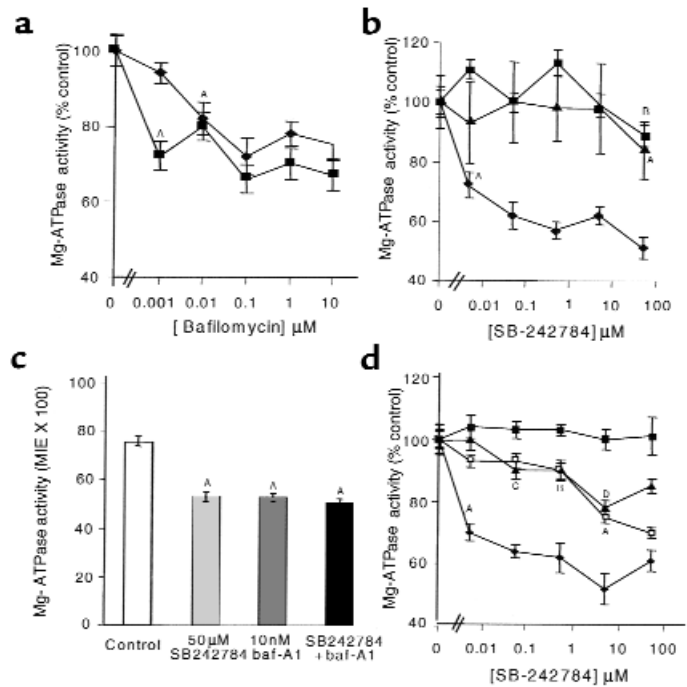
Experimental protocol. Adult female Sprague-Dawley rats weighing 250 g were divided into six groups of eight animals each: groups 1–3 (controls) had free access to tap water; groups 4–6 (acid-loaded rats) had free access to drinking water containing 280 mM (1.5%) NH₄Cl plus 1% sucrose, for 8 days. All rats were fed with a standard rodent laboratory diet (Mucedola 4RF21; Settimo Milanese). The diet contained 1,260 IU/kg vitamin D₃, and estrogen was absent. Volume, pH and total acidity of urine, and water intake were monitored daily. At day 2, when acid-loaded rats presented a stable acidosis, all groups were treated orally with vehicle (groups 1 and 4), SB 242784 at 5 mg/kg (groups 2 and 5), and SB 242784 at 10 mg/kg (groups 3 and 6).

Measurements of urine total acidity. Free acidity was evaluated by titrating urine samples with 0.01 M NaOH at pH 7.4. NH₄⁺ content was determined by enzymatic bioanalysis (Boehringer Ammonia Kit). Total acidity of urine was measured as the sum of free acidity and ammonium content and is expressed in equivalents per liter (*N*).

Measurements of ammonium balance. Ammonium balance was calculated by dividing the urinary NH₄⁺ output by the daily NH₄⁺ intake, both expressed as milliequivalents per day.

Figure 2

Effects of SB 242784 on the activity of total Mg^{2+} -ATPase activity. Results are expressed as $MIE \times 100 \pm SEM$. (a) Effect of bafilomycin- A_1 (baf- A_1 , squares) and SB 242784 (diamonds); $^A P < 0.001$ versus control (lowest concentration achieved). (b) Effect of SB242784 on osteoclast Mg^{2+} -ATPase activity, KPC cells (squares), and liver hepatocytes (triangles). $^A P < 0.001$ versus control; $^B P < 0.05$ versus control. (c) Additive effects of bafilomycin and SB 242784 on Mg^{2+} -ATPase activity in human osteoclasts. $^A P < 0.001$ versus control. (d) Effects of SB 242784 on Mg^{2+} -ATPase activity in human osteoclasts (diamonds), cynomolgus monkey (CM) KPC cells (open squares), CM microglial cells (brain, triangles), and CM liver hepatocytes (closed squares). $^A P < 0.001$, $^B P < 0.05$, $^C P < 0.02$, $^D P < 0.005$, all versus control.



Statistical analysis

In situ cytochemical Mg^{2+} -ATPase assay and histomorphometry. Statistical analysis was done by an unpaired t test (two-tailed).

Hypercalcemia induced by the retinoid Ro 13-6298 in TPTX rats and osteoporosis induced by ovariectomy in rats. Statistical analysis was performed using RS1/Explore programs (BBN Software Products, Cambridge, Massachusetts, USA). Data were expressed as the mean plus or minus standard error for each group. Analysis of all parameters were based on two-way ANOVA. When significant differences were indicated, effects of treatments were compared by a multicompare procedure. A P value lower than 0.05 was considered significant.

Results

Inhibition of $V-H^+$ -ATPase in situ

Selectivity studies. This assay allows the quantitation of ATPase activity in individual cells in situ and was used to estimate the relative effects of SB 242784 on $V-H^+$ -ATPase in several human and cynomolgus monkey tissues. As discussed in Methods, the assay relies on the use of the phosphate-trapping agent LACA complex, precluding the use of undecalcified sections of human and monkey bone. To address this, osteoclast $V-H^+$ -ATPase activity was assayed in multiple sections from six different osteoclastomas. V -ATPase activity was inhibited by bafilomycin in a dose-dependent manner (Figure 2a). Based on bafilomycin sensitivity, approximately 25% of the Mg^{2+} -ATPase activity was $V-H^+$ -ATPase in osteoclasts and kidney proximal convoluted (KPC) tubule cells (Figure 2a). The remaining activity represents microsomal/mitochondrial bafilomycin-insensitive Mg^{2+} -ATPase(s).

For each concentration of SB 242784 tested (0–50 μM), serial sections were assayed in the presence of 10 nM bafilomycin (estimated 100% inhibition of $V-H^+$ -ATPase) and 10 nM bafilomycin plus 50 μM SB 242784 (to ascertain whether SB 242784 inhibited a bafilomycin-insensitive component). Human osteoclast Mg^{2+} -ATPase was potently inhibited by SB 242784 (Figure 2b). Based on bafilomycin sensitivity (estimated maximum inhibition at 10 nM), the osteoclast $V-H^+$ -ATPase was significantly inhibited by SB 242784 with an estimated IC_{50} less than 5 nM. The effects of SB 242784 on $V-H^+$ -ATPase activity in human KPC tubule cells and liver hepatocytes are also shown in Figure 2b. Kidney and liver cells demonstrated no concentration-dependent inhibition up to 5 μM , but demonstrated 40% and 80% inhibition, respectively, at the maximum concentration of 50 μM . Comparison between giant cell tumor,

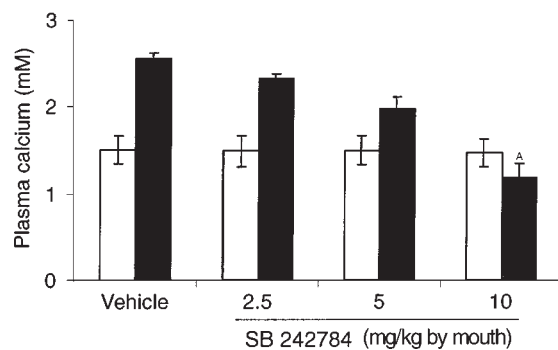


Figure 3

Effect of SB 242784 on retinoid-induced hypercalcemia in TPTX rats ($n = 8$). Open bars, basal value; filled bars, SB 242784; $^A P < 0.01$ versus vehicle.

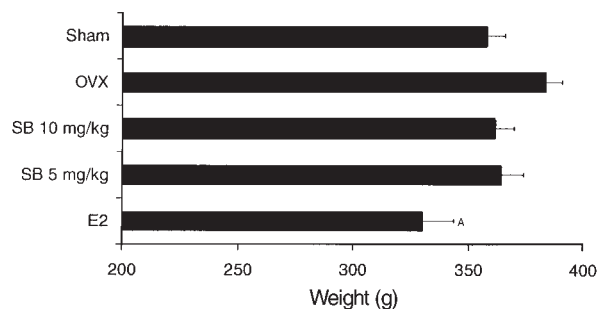


Figure 4
Effect of estrogen (E2) and SB 242784 on body weight of OVX rats at the end of the 6-month treatment. ^A*P* < 0.01 versus OVX-vehicle.

spleen, and stomach cell types revealed a similar profile of osteoclast selectivity (not shown). Osteoclasts demonstrating no bafilomycin-sensitive ATPase activity were unaffected by SB 242784 (not shown). In all cell types, SB 242784 had no effect on bafilomycin-insensitive ATPase activity and therefore no effect on other Mg²⁺-ATPases (osteoclast V-ATPase shown as representative; Figure 2c).

SB 242784 inhibited V-H⁺-ATPase in monkey KPC tubule cells and brain microglial cells at an IC₅₀ of approximately 5 μM (Figure 2d). SB 242784 had no effect on V-H⁺-ATPase activity in cynomolgus monkey liver hepatocytes, brain granular cells (Figure 2d), or liver endothelial cells (not shown). In all cell types, SB 242784 had no effect on bafilomycin-insensitive ATPase activity (not shown).

To characterize further the selectivity of action of this compound against other enzymes that are known to be involved in the process of bone resorption, SB 242784 was tested against a number of MMPs and cathepsins. Only very low inhibitory activity was observed, with an IC₅₀ of 5 μM for MMP-9 and human cathepsin S. No activity (IC₅₀ > 10 μM) was displayed for MMP-2, human and rat cathepsin K, or human cathepsin L (data not shown).

Effect of SB 242784 on retinoid-induced hypercalcemia in TPTX rats

It is well-known that excess vitamin A leads to an increase of osteoclastic bone resorption and of the number of osteoclasts. Ro 13-6298 is one of the most potent retinoids known, and it induces a stimulation of bone resorption in the TPTX rat. The changes in bone resorption can be monitored by measuring plasma calcium levels (14).

In our experiments subcutaneous injections of 30 μg/rat/d of Ro 13-6298 for 3 days in control TPTX rats caused a significant increase in plasma calcium levels from 1.51 ± 0.16 to 2.55 ± 0.07 mM (*P* < 0.01). Oral administration of 2.5, 5, and 10 mg/kg of SB 242784 caused dose-related inhibition of retinoid-induced hypercalcemia of 20% (not significant), 54% (not significant), and 128% (*P* < 0.01), respectively (Figure 3).

Effect of SB 242784 in ovariectomized rats

In a previous experiment performed in adult (8-month-old) ovariectomized (OVX) rats for 3 months (18), SB 242784 caused statistically significant prevention of the decrease of BMD at the orally administered dose of 10 mg/kg/d, but not at the lower doses of 1 or 3 mg/kg/d. Therefore, in this 6-month experiment, the doses of 5 and 10 mg/kg/d of SB 242784, given by mouth, were chosen for the treatment of OVX rats.

Body weight gain in all groups was monitored throughout the whole experimental period to obtain an indication of possible overt toxic effects of SB 242784. As may be observed in Figure 4, where the body weight of animals at the end of the 6-month experimental period is reported, only estrogen but not SB 242784 treatment caused a statistically significant decrease of weight gain.

BMD of distal femur metaphysis. Assessment of BMD by dual-photon absorptiometry (DEXA) clearly showed that ovariectomy induced a marked, continuous, and significant decrease in femur BMD between the first and the sixth month after surgery (Figure 5a). As expected, the reference compound 17β-estradiol, administered as 2.5-mg pellets implanted subcuta-

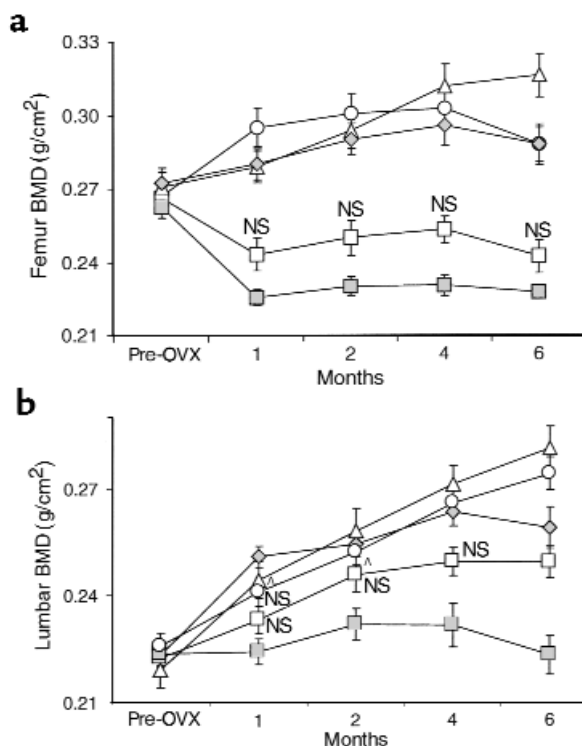


Figure 5
Effect of SB 242784 on BMD of distal femur metaphysis (a) and lumbar vertebrae L3-L4 (b) in OVX rats, *n* = 10. Filled diamonds, sham-operated rats treated with vehicle; open circles, estradiol; open squares, SB 242784 5 mg/kg; open triangles, SB 242784 10 mg/kg; closed squares, OVX-vehicle. All points were statistically different from OVX-vehicle at *P* < 0.01, except when otherwise indicated: ^A*P* < 0.05. NS, not statistically different from OVX-vehicle.

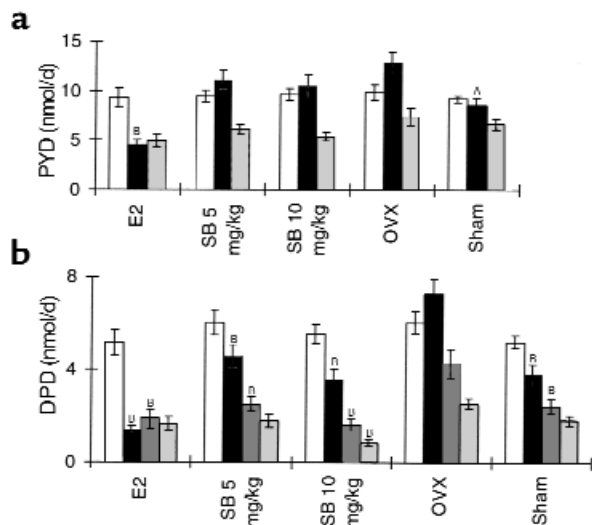


Figure 6
Effect of SB 242784 on total urinary excretion of PYD (a) and DPD (b) cross-links in OVX rats, $n = 10$. Open bars, pre-OVX basal value; filled bars, 1 month; dark-gray bars, 2 months; light-gray bars, 3 months. ^A $P < 0.05$; ^B $P < 0.01$ versus OVX-vehicle.

neously, caused a significant protective effect on BMD at all the time points assessed. Similarly, SB 242784 at the higher dose of 10 mg/kg/d fully prevented the decrease of BMD throughout the experimental period. At the lower dose of 5 mg/kg, SB 242784 maintained a BMD of the femur metaphysis slightly higher than in vehicle-treated OVX rats for all the 6 months. This difference, however, did not reach the statistical significance at any time point.

BMD of lumbar vertebrae (L3–L6). Contrary to what occurred in the femoral metaphysis, the effect of ovariectomy in these growing animals was to prevent the age-related increase of BMD of lumbar vertebrae observed in sham-operated rats. OVX animals treated with estradiol or 10 mg/kg SB 242784 showed the same increase of bone density as observed in the sham-operated group during the whole experimental period (Figure 5b). Also the lower dose of 5 mg/kg of SB 242784 caused an increase of spine BMD that was statistically significant at months 5 and 6.

Total urinary PYD and DPD. In comparison with sham-operated animals, ovariectomy caused significant increases ($P < 0.01$) in total urinary levels of PYD at

month 1 and of DPD at months 1 and 2 after surgery, with a peak effect at the first month (Figure 6). These increases were completely and significantly ($P < 0.01$) prevented by estradiol administration. SB 242784, at 5 and 10 mg/kg/d, fully and significantly ($P < 0.01$) inhibited DPD increase ovariectomy induced at months 1 and 2 after surgery; at the highest dose of 10 mg/kg, effect was also observed at month 3. Urinary PYD levels were not significantly modified by this compound.

Urine volume, pH, and total acidity. In comparison with sham-operated animals, OVX rats, treated with vehicle or SB 242784, did not show any differences in urine volume, pH, and total acidity at all time points. Conversely, estradiol induced significant increases ($P < 0.01$) in urine volume from the second to the sixth month and in total acidity at months 2 and 3 (data not shown).

Histomorphometry. The effects of OVX, estradiol, and SB 242784 on cancellous bone volume and architecture at the proximal tibia are shown in Figure 7, a–d. Trabecular number was significantly lower (47%) in OVX rats relative to sham controls (Figure 7a), resulting in a significant decrease (50%) in trabecular area (Figure 7b). However, there was no effect of OVX on trabecular thickness (not shown), and the apparent increase (58%) in trabecular spacing did not reach significance. The OVX-induced loss in trabecular number and percentage of trabecular area was prevented by estradiol and SB 242784 at the higher dose (i.e., not significantly different from sham controls; Figure 7, a and b). At the lower dose of 5 mg/kg, SB 242784 had no effect on any parameter. Trabecular spacing was also significantly reduced in the rats treated with estradiol (74%; $P < 0.05$ versus OVX) and SB 242784 at 10 mg/kg (84%; $P < 0.03$ versus OVX) relative to the sham group.

Figure 7
Effects of SB 242784 on histomorphometric parameters in OVX rats ($n = 10$). Results are presented as mean \pm SEM. (a) Trabecular bone number. ^A $P < 0.005$ versus sham, ^B $P < 0.0075$ versus OVX, ^C $P < 0.0002$ versus OVX. NS, not significantly different from OVX. (b) Percentage of trabecular area. ^A $P < 0.004$ OVX versus sham, and Est (estradiol) versus OVX, ^C $P < 0.0003$ versus OVX. NS, not significantly different from OVX. (c) Percentage of eroded perimeter; NS (OVX vs. sham and SB 242784-5 vs. OVX). ^B $P < 0.0383$, Est versus OVX, and $P < 0.0518$, SB 242784 versus OVX. (d) Percentage of osteoid perimeter.

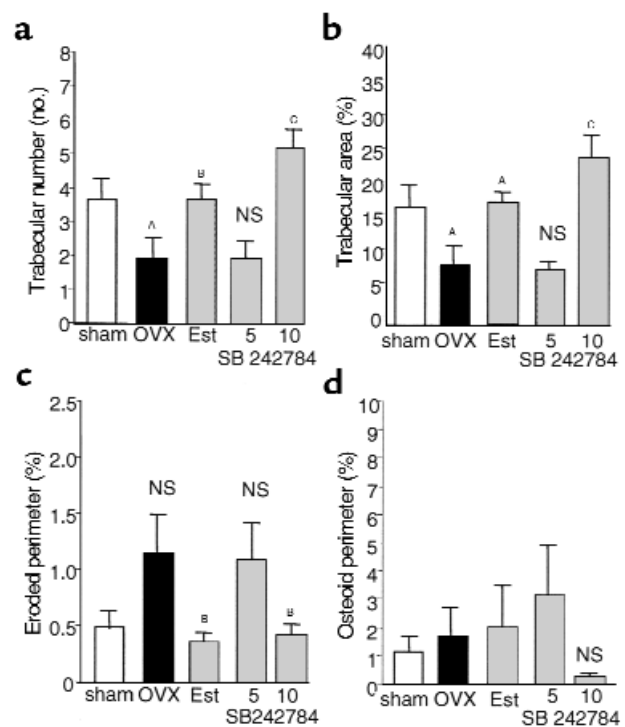


Figure 8

Photomicrographs of trabecular bone area in the proximal tibia of sham-operated (a), OVX (b), and OVX animals treated with estrogen (c) and SB 242784 10 mg/kg (d) for 6 months.

Percentage of eroded perimeter (Figure 7c) was 133% higher in the OVX group relative to sham and was normalized (equivalent to sham) by both estradiol (67% lower) and SB 242784 at 10 mg/kg (62% lower). Although overall bone turnover is generally increased in OVX-induced bone loss (19, 20), in this long-term study bone formation rates (BFR/BV, TV, BS) were low and equivalent in the OVX and sham groups (not shown). BFR/BV and BFR/TV were 70% ($P < 0.04$) and 72% ($P < 0.04$) lower in the SB 242784 at 10 mg/kg group, respectively, relative to sham (but not significantly different to OVX). The mineral apposition rate was comparable in all groups. Percentage of osteoid perimeter was comparable between OVX and sham animals and not affected (although data were highly variable) by estradiol or SB 242784 (Figure 7d).

In summary, bone resorption (and overall bone remodeling) was significantly decreased by SB 242784 at 10 mg/kg, with a significant net gain in bone volume. Figure 8 shows photomicrographs of trabecular bone area in the proximal tibia of sham-operated, OVX and OVX animals treated with SB 242784 at 10 mg/kg for 6 months.

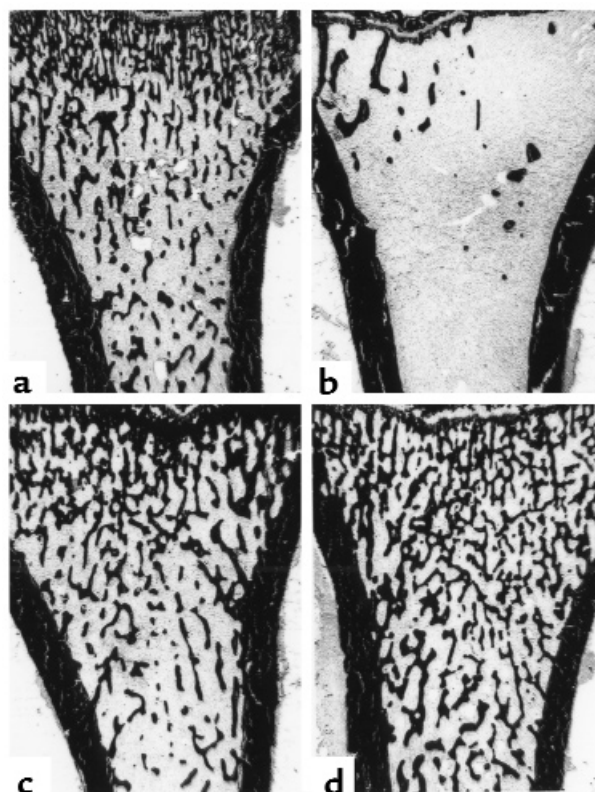
Effects of SB 242784 in acid-loaded rats

Treatment with vehicle or SB 242784, at 5 or 10 mg/kg, administered by mouth, had no effect on urine pH (data not shown) and total acid concentration (Figure 9) in both control and acid-loaded animals. In addition, the same treatments in acid-loaded animals caused no significant change of ammonium balance, i.e., the ratio between the amount of ammonium excreted in urine and the amount of ammonium taken with drinking water (Figure 10). Ammonium intake with food accounts for the values greater than 1 for this ratio.

Discussion

Acidification of the resorbing compartment is one of the most important features of osteoclast biological activity in the process of bone resorption: the acidic environment is absolutely required for the degradation of both inorganic and organic components of bone (3). The lowering of pH in the bone-resorbing compartment is accomplished by a high concentration of vacuolar-type proton pumps (V-H⁺-ATPases) on the apical pole of the cell (ruffled border).

It has been shown that expression of the proton channel part of V-H⁺-ATPase is stimulated in resorbing osteoclasts (21) and that antisense RNA and DNA molecules targeted against two subunits of the V-H⁺-ATPase do indeed inhibit bone resorption by rat osteoclasts (22). This enzyme is therefore a major potential target for reducing osteoclast activity and, consequently, for design-



ing novel agents useful for the treatment of osteoporosis.

Proton-translocating V-H⁺-ATPases (5, 23) are ubiquitous components of eukaryotic organisms and are the major electrogenic pumps of vacuolar membranes. The V-H⁺-ATPases pump protons from the cytoplasm to the lumen using the energy released by ATP hydrolysis. The electrical potential difference created across the membrane is used to drive the movement of ions and solutes into the vacuole. Given the ubiquitous nature of vacuolar proton pumps, therapeutically useful V-H⁺-ATPase inhibitors would need to be able to discriminate between the osteoclast enzyme and the other essential V-H⁺-ATPases.

Although sequence differences between the subunits of V-H⁺-ATPases of different origins have been reported, the existence of biochemically distinct isoforms of the enzyme have not been demonstrated until very recently. Previously, discordant evidence has appeared in the literature, either supporting or rejecting the existence of an isoform of enzyme uniquely expressed in the plasma membrane of the osteoclasts. Whereas osteoclasts do express the ubiquitous subunits B2 (24, 25) and C-E (26), “osteoclast-specific” 67-kD subunit A (27, 28) and 116-kD (29) subunits were described, which, however, were subsequently shown to be ubiquitously expressed in human tissues (30, 31). Also, the “peculiar sensitivity” of chicken osteoclast V-ATPase to vanadate (32) and to nitrate (33) has not been confirmed by independent investigators in either chicken (4, 34, 35) or mammalian (36) osteoclasts.

Very recently, however, the existence of a specific osteoclast 116-kD (OC-116 kD) subunit has been con-

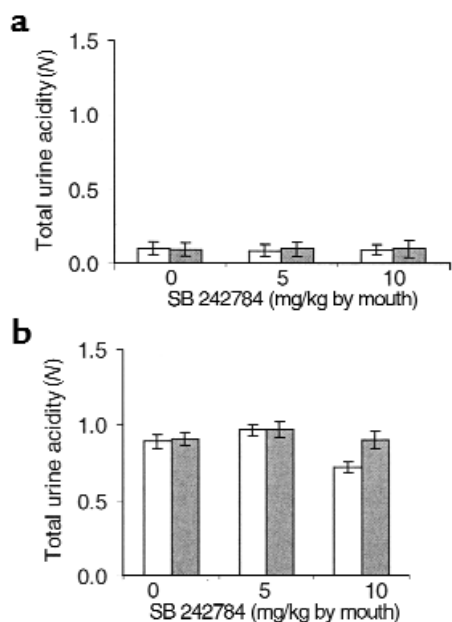


Figure 9 Effect of SB 242784 on urinary total acidity (N) in rats drinking tap water (a) or 1.5% NH₄Cl plus 1% sucrose (b). No statistically significant difference was observed before (open bars) or 24 hours after (filled bars) the treatment.

firmed by in situ hybridization and sequence analysis (37). Knockout mice with a null mutation in the *ATP6i* gene, coding for the OC-116 kD subunit were growth retarded and developed severe osteopetrosis (38). Heterozygous animals appeared normal. Histological analysis of the OC-116 kD^{-/-} mice revealed long-bone abnormalities manifested as the absence of marrow cavities and expanded growth plates with an extended zone of calcified cartilage. Enzyme histochemical analysis showed that OC-116 kD^{-/-} mice have a normal number of osteoclasts that attach to bone but do not form resorption lacunae. Importantly, OC-116 kD^{-/-} mice had normal acid-base balance of blood and urine and functional intracellular acidification, illustrating that OC-116 kD-null mutation is unlikely to affect V-ATPase of lysosomes/endosomes and kidney tubule cells. From all these data it appears that the osteoclast 116 kD is structurally and functionally different from the corresponding subunits in other V-ATPases.

Starting from bafilomycin A₁, a potent inhibitor of all the V-H⁺-ATPases, we were able to design a novel class of compounds with strong V-H⁺-ATPase-inhibitory activity and possessing a clear-cut selectivity for the osteoclast enzyme. The most representative compound of the class is SB 242784, whose in vitro V-H⁺-ATPase inhibitory profile has been reported previously (11). SB 242784 is a low-nanomolar inhibitor (IC₅₀ = 26.3 nM) of the bafilomycin-sensitive (vacuolar) Mg²⁺-ATPase in membrane preparations of osteoclast obtained from egg-laying hens. In addition, SB 242784 was a very potent inhibitor of bone resorption (IC₅₀ = 3.4 nM) in an assay measuring the collagen fragments released from bone slices after 48-

hour incubation with human osteoclasts. Although there is no reason to believe that the expression of any of the ATPase subunits is affected by SB 242784, this possibility has not been ruled out experimentally.

In this paper we have further characterized this compound with regard to its selectivity for the human osteoclast enzyme when compared with other V-H⁺-ATPases in different human tissues. Using an in situ cytochemical assay capable of measuring ATPase activity in single cells, it was possible to demonstrate that SB 242784 has greater than 1,000-fold selectivity for the osteoclast V-H⁺-ATPase compared with the enzyme measured in kidney, liver, spleen, stomach, brain, or endothelial cells. It has no effect on other cellular ATPases. The molecular mechanism by which SB 242784 exerts its selectivity is poorly understood. The lipophilic nature of this compound might suggest an interaction with one or more components of the integral membrane domain, for example, the 116-kD subunit for which different isoforms have been identified in human (29) and rabbit osteoclasts (37, 39) or the 16-kD proteolipid, whose sequence in human osteoclast is still unknown and for which several genes have been identified in the human genome (40). In any case specific studies on the interaction of SB 242784 with the enzyme subunits are required to precisely identify the protein target of this class of inhibitors.

The observed in vitro antiresorptive activity of SB 242784 is unlikely to be due to its action on different enzymes that are known to be involved in the bone-resorption process; this is supported by its very low or no inhibitory activity against a series of MMPs or cathepsins that were inhibited by SB 242784 only at concentrations of 5 μM or higher.

When tested in animal models of bone resorption in vivo, SB 242784 inhibited bone resorption in both acute and chronic models in the rat. Retinoid Ro 13-6298 induced a stimulation of bone resorption with a consequent increase in calcium plasma levels in TPTX rats (14). In this acute model, oral administration of SB 242784 for 3 days inhibited, in a dose-related way, the retinoid-induced hypercalcemia, with complete prevention at the higher dose of 10 mg/kg.

Bone loss induced by ovariectomy in rats and postmenopausal bone loss present similar characteristics,

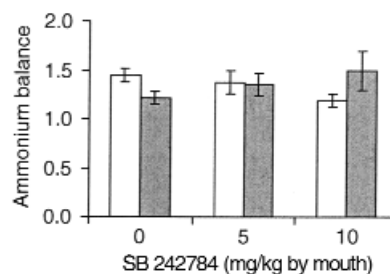


Figure 10 Effect of SB 242784 on the ratio between ammonium excreted in urine and ammonium taken in with drinking water in acid-loaded rats. Open bars, before treatment; filled bars, 24 hours after treatment.

such as increased rate of bone turnover with resorption exceeding formation, an initial rapid phase of bone loss followed by a slower phase, greater loss of cancellous than cortical bone, decreased intestinal absorption of calcium, and similar skeletal response to therapy with estrogen. All these similarities provide strong evidence that the OVX rat bone-loss model is suitable for studying problems that are relevant to postmenopausal bone loss (41). In this animal model chronic treatment for 6 months with 10 mg/kg/d of SB 242784 by mouth fully prevented the decrease in BMD induced by ovariectomy in the femur and lumbar spine throughout the treatment period. The decrease of BMD in the lumbar spine was significantly reduced also with the lower dose of 5 mg/kg/d of this compound administered orally at months 5 and 6.

Bone constitutes the major pool of PYD and DPD cross-links. Although quantities of DPD have been detected in soft tissues such as the aorta and ligaments (42), the turnover of collagen in these tissues is very low, and thus urinary DPD can be considered to be a specific marker for bone-collagen degradation (43, 44). Two studies have demonstrated the close association between urinary cross-link excretion and the rate of bone resorption, as determined by radioisotopic and histomorphometric measurements. It is generally accepted that these cross-links, as measured in the urine, reflect bone resorption (45). Urinary DPD levels were significantly reduced with both doses of SB 242784 at months 1 and 2, and, at the higher dose of 10 mg/kg/d, this effect was evident also at month 3. Contrary to estrogen and sham groups, no significant modification in PYD levels were observed in SB 242784-treated groups. These biochemical indices were consistent with a partial suppression of the increase in bone turnover that follows ovariectomy.

Static and dynamic histomorphometry of the proximal tibia confirmed that SB 242784, at the higher dose of 10 mg/kg/d, prevented the OVX-induced loss in trabecular number and area. The antiresorptive mechanism of action of SB 242784 was confirmed by the significant reduction in the extent of eroded surfaces (percentage of Er.Pm) and bone turnover (BFR/BV).

The 6-month treatment with 5 or 10 mg/kg/d of SB 242784 caused no overt toxic effect in OVX rats. They behaved normally during the whole experimental period, and their weight at the end of treatment was not statistically different from that of OVX rats treated with vehicle. As expected, estrogen replacement significantly decreased body weight. However, it should be noted that other V-H⁺-ATPase-dependent processes were not explicitly studied, so complete specificity cannot be claimed.

During this study, the possible effect of the treatment on renal V-H⁺-ATPase was also monitored by measuring the volume, pH, and total acidity of the urine. It is known, in fact, that a V-H⁺-ATPase in the intercalated cells of convoluted tubules is responsible for urinary acidification and bicarbonate reabsorption.

As predicted by in vitro data, no effect of SB 242784 was observed in the treated animals when compared with controls, confirming, also in vivo, its selectivity for the osteoclast enzyme.

To further confirm the lack of effect of SB 242784 on urinary acidification by kidney V-H⁺-ATPase, an acid-loaded model was set up that could better detect any possible effect. It is known that response to acid loading in rats involves transport of large amounts of V-H⁺-ATPase from the cytoplasmic vesicles to plasma membranes (46), where it is crucial for the maintenance of urinary pH.

Urinary acid output increased by about 10-fold in animals drinking a solution containing 1.5% ammonium chloride and 1% sucrose (Figure 9b), as compared with animals drinking water (Figure 9a). However, treatment with 5 or 10 mg/kg/d of SB 242784 did not affect total acid output (Figure 9) or urine pH (data not shown). Also, the animals treated with SB 242784 were able to excrete all the ammonium load in a manner similar to vehicle-treated rats (Figure 10).

In summary, all endpoints measured demonstrated outstanding efficacy of SB 242784 in the prevention of ovariectomy-induced bone loss, including BMD, biochemical markers of bone resorption, and histomorphometry. There were no overt adverse effects of administration of SB 242784 to rats for 6 months, including a lack of effect on kidney function or urine acidification. These studies clearly define the osteoclast V-ATPase as an excellent target for antiresorptive therapy for osteopenic disorders such as osteoporosis.

Acknowledgments

The authors would like to thank A. Volontieri, R. Mariani, H. Minehart, and G. Beltramea for expert technical assistance. Anne Romanic performed the MMP assays and Ted Tomaszek the cathepsin assays.

1. Dempster, D.W., and Lindsay, R. 1993. Pathogenesis of osteoporosis. *Lancet*. **341**:797–801.
2. Baron, R., Neff, L., Louvard, D., and Courtoy, P.J. 1985. Cell-mediated extracellular acidification and bone resorption: evidence for a low pH in resorbing lacunae and localization of a 100 kD lysosomal membrane protein at the osteoclast ruffled border. *J. Cell Biol.* **101**:2210–2222.
3. Hall, T.J., and Chambers, T.J. 1996. Molecular aspects of osteoclast function. *Inflamm. Res.* **45**:1–9.
4. Blair, H.C., Teitelbaum, S.M., Ghiselli, R., and Gluck, S. 1989. Osteoclastic bone resorption by a polarized vacuolar proton pump. *Science*. **245**:855–857.
5. Finbow, E.F., and Harrison, M.A. 1997. The vacuolar H⁺-ATPase: a universal proton pump of eukaryotes. *Biochem. J.* **324**:697–712.
6. Bowmann, E.J., Siebers, A., and Altendorf, K. 1988. Bafilomycin: a class of inhibitors of membrane ATPases from microorganisms, animal cells, and plant cells. *Proc. Natl. Acad. Sci. USA*. **85**:7972–7976.
7. Sundquist, K., Lakkakorpi, P., Wallmark, B., and Vaananen, K. 1990. Inhibition of osteoclast proton transport by bafilomycin A₁ abolishes bone resorption. *Biochem. Biophys. Res. Commun.* **168**:309–313.
8. Farina, C., et al. 1995. Bafilomycin A₁ inhibits bone resorption in vivo after systemic administration. *J. Bone Miner. Res.* **10**(Suppl. 1):S296. (Abstr.)
9. Keeling, D.J., Herslof, M., Mattsson, J.P., and Ryberg, B. 1998. Tissue-selective inhibition of vacuolar acid pumps. *Acta Physiol. Scand.* **643**:195–201.
10. Gagliardi, S., et al. 1998. 5-(5,6-Dichloro-2-indolyl)-2-methoxy-2,4-pentadienamides: novel and selective inhibitors of the vacuolar H⁺-ATPase of osteoclasts with bone antiresorptive activity. *J. Med. Chem.* **41**:1568–1573.
11. Nadler, G., et al. 1998. (2Z,4E)-5-(5,6-Dichloro-2-indolyl)-2-methoxy-N-(1,2,2,6,6-pentamethylpiperidin-4-yl)-2,4-pentadienamide, a novel, potent and selective inhibitor of the osteoclast V-ATPase. *Bioorg. Med. Chem. Lett.* **24**:3621–3626.

12. Chayen, R., et al. 1981. The use of a hidden metal-capture reagent for the measurement of Na⁺-K⁺-ATPase activity: a new concept in cytochemistry. *Histochemistry*. **71**:533-541.
13. Trechsel, U., Stutzer, A., and Fleisch, H. 1987. Hypercalcemia induced with an arotinoid in thyroparathyroidectomized rats. *J. Clin. Invest.* **80**:1679-1686.
14. Loeliger, P., Bollag, W., and Mayer, H. 1980. Arotinoids, a new class of highly active retinoids. *Eur. J. Med. Chem. - Chim. Ther.* **15**:9-15.
15. Wronski, T.J., Cintron, M., Doherty, A.L., and Dann, L.M. 1988. Estrogen treatment prevents osteopenia and depresses bone turnover in ovariectomized rats. *Endocrinology*. **123**:681-686.
16. Wronski, T.J., Yen, C.F., and Scott, K.S. 1991. Estrogen and diphosphonate treatment provide long-term protection against osteopenia in ovariectomized rats. *J. Bone Miner. Res.* **6**:387-394.
17. Eyre, D.R., Koob, T.J., and Van Ness, K.P. 1984. Quantitation of hydroxy-pyridinium cross links in collagen by high-performance liquid chromatography. *Anal. Biochem.* **137**:380-388.
18. Farina, C., et al. 1997. An orally active, selective inhibitor of the osteoclast V-H⁺-ATPase, prevents bone loss in both growing and mature ovariectomized rats. *J. Bone Miner. Res.* **12**(Suppl. 1):S478. (Abstr.)
19. Jerome, C.P., et al. 1994. Bone functional changes in intact, ovariectomized, and ovariectomized, hormone-supplemented adult cynomolgus monkeys (*Macaca fascicularis*) evaluated by serum markers and dynamic histomorphometry. *J. Bone Miner. Res.* **9**:527-540.
20. Yamamoto, M., et al. 1998. The integrin ligand echistatin prevents bone loss in ovariectomized mice and rats. *Endocrinology*. **139**:1411-1419.
21. Laitala, T., and Vaananen, H.K. 1993. Proton channel part of vacuolar H⁽⁺⁾-ATPase and carbonic anhydrase II expression is stimulated in resorbing osteoclasts. *J. Bone Miner. Res.* **8**:119-126.
22. Laitala, T., and Vaananen, H.K. 1994. Inhibition of bone resorption in vitro by antisense RNA and DNA molecules targeted against carbonic anhydrase II or two subunits of vacuolar H⁽⁺⁾-ATPase. *J. Clin. Invest.* **93**:2311-2318.
23. Forgac, M. 1996. Regulation of vacuolar acidification. *Soc. Gen. Physiol. Ser.* **51**:121-132.
24. Lee, B.S., Holliday, L.S., Ojikutu, B., and Gluck, S.L. 1996. Osteoclasts express the B2 isoform of vacuolar H⁽⁺⁾-ATPase intracellularly and on their plasma membranes. *Am. J. Physiol.* **270**:C382-C388.
25. Mattsson, J.P., et al. 1997. Characterization and cellular distribution of the osteoclast ruffled membrane vacuolar H⁺-ATPase B-subunit using isoform-specific antibodies. *J. Bone Miner. Res.* **12**:753-760.
26. Van Hille, B.V., Vanek, M., Richener, H., Green, J.R., and Bilbe, G. 1993. Cloning and tissue distribution of subunits C, D, and E of the human vacuolar H⁽⁺⁾-ATPase. *Biochem. Biophys. Res. Commun.* **197**:15-21.
27. Hernandez, N., Bartkiewicz, M., Collin-Osbody, P., Osbody, P., and Baron, R. 1995. Alternative splicing generates a second isoform of the catalytic A subunit of the vacuolar H⁽⁺⁾-ATPase. *Proc. Natl. Acad. Sci. USA.* **92**:6087-6091.
28. Van Hille, B., Richener, H., Evans, D.B., Green, J.R., and Bilbe, G. 1993. Identification of two subunit A isoforms of the vacuolar H⁽⁺⁾-ATPase in human osteoclastoma. *J. Biol. Chem.* **268**:7075-7080.
29. Li, Y.P., Chen, W., and Stashenko, P. 1996. Molecular cloning and characterization of a putative novel human osteoclast-specific 116-kD vacuolar proton pump subunit. *Biochem. Biophys. Res. Commun.* **218**:813-821.
30. Van Hille, B., Richener, H., Green, J.R., and Bilbe, G. 1995. The ubiquitous VA68 isoform of subunit A of the vacuolar H⁽⁺⁾-ATPase is highly expressed in human osteoclasts. *Biochem. Biophys. Res. Commun.* **214**:1108-1113.
31. Scott, B.B., and Chapman, C.G. 1998. The putative 116 kD osteoclast specific vacuolar proton pump subunit has ubiquitous tissue distribution. *Eur. J. Pharmacol.* **346**:R3-R4.
32. Chatterjee, D., et al. 1992. Sensitivity to vanadate and isoforms of subunits A and B distinguish the osteoclast proton pump from other vacuolar ATPases. *Proc. Natl. Acad. Sci. USA.* **89**:6257-6261.
33. Chatterjee, D., Neff, L., Chakraborty, M., Fabricant, C., and Baron, R. 1993. Sensitivity to nitrate and other oxyanions further distinguishes the vanadate-sensitive osteoclast proton pump from other vacuolar ATPases. *Biochemistry*. **32**:2808-2812.
34. Mattsson, J.P., et al. 1993. Isolation and reconstitution of a vacuolar-type proton pump of osteoclast membranes. *Biochem. Biophys. Acta.* **1146**:106-112.
35. Mattsson, J.P., Lorentzon, P., Wallmark, B., and Keeling, D.J. 1994. Characterization of proton transport in bone-derived membrane vesicles. *J. Biol. Chem.* **269**:24979-24982.
36. Hall, T.J., and Schaeuble, M. 1994. A pharmacological assessment of the mammalian osteoclast vacuolar H⁺-ATPase. *Bone Miner.* **27**:159-166.
37. Manolson, M.F., Landolt-Marticorena, C., Yu, H., Williams, K.M., and Heersche, J. 1999. Topology and function of the 116 kD V-ATPase subunit in osteoclasts and yeast. *J. Bone Miner. Res.* **14**(Suppl. 1):S484. (Abstr.)
38. Li, Y.P., Chen, W., Lieng, Y., Li, E., and Stashenko, P. 1999. ATP6i-deficient mice exhibit severe osteopetrosis due to loss of osteoclast-mediated extracellular acidification. *Nat. Genet.* **23**:447-451.
39. Yu, E., Chen, W., Lees, R., Heersche, J., and Manolson, M.F. 1998. Identification of vacuolar-type proton-ATPase subunits unique to osteoclasts. *Bone*. **23**(Suppl.):S549. (Abstr.)
40. Hasebe, M., Hanada, H., Moriyama, Y., Maeda, M., and Furai, M. 1992. Vacuolar type H⁺-ATPase genes: presence of four genes including pseudogenes for the 16-kD proteolipid subunit in the human genome. *Biochem. Biophys. Res. Commun.* **183**:856-863.
41. Kalu, D.N. 1991. The ovariectomized rat model of postmenopausal bone loss. *Bone Miner.* **25**:175-192.
42. Robins, S.P., Duncan, A., and Riggs, B.L. 1990. Direct measurement of free hydroxy-pyridinium crosslinks of collagen in urine as new markers of bone resorption in osteoporosis. In *Osteoporosis*. C. Christiansen and K. Overgaard, editors. Osteopress. Copenhagen, Denmark. 465-468.
43. Eastell, R., Colwell, A., Hampton, L., and Reeve, J. 1997. Biochemical markers of bone resorption compared with estimates of bone resorption from radiotracer kinetic studies in osteoporosis. *J. Bone Miner. Res.* **12**:59-65.
44. Delmas, P.D., Schlemmer, A., Gineyts, E., Riis, B., and Christiansen, C. 1991. Urinary excretion of pyridinoline crosslinks correlates with bone turnover measured on iliac crest biopsy in patient with vertebral osteoporosis. *J. Bone Miner. Res.* **6**:639-644.
45. Siebel, M.J., Robins, S.P., and Bilezikian, J.P. 1992. Urinary pyridinium crosslinks of collagen. Specific markers of bone resorption in metabolic bone disease. *Trends Endocrinol. Metab.* **3**:263-270.
46. Bastani, B., Purcel, H., Hemken, P., Trigg, D., and Gluck, S. 1991. Expression and distribution of renal vacuolar proton-translocating adenosinetriphosphatase in response to chronic acid and alkali loads in the rat. *J. Clin. Invest.* **88**:126-136.